Pathway and Kinetics of Cylinder-to-Sphere Order−Order Transition in Block Copolymers

R. Krishnamoorti* and M. A. Modi

Department of Chemical Engineering, University of Houston, Houston, Texas 77204-4792

M. F. Tse and H.-C. Wang

Exxon Chemical Company, 5200 Bayway Drive, Baytown, Texas 77521

Received November 1, 1999; Revised Manuscript Received March 6, 2000

ABSTRACT: The pathway and kinetics for the cylinder-to-sphere order−order transition in a mixture of a matched diblock and triblock copolymer of styrene and ethylene−butene-1 is reported. The microstructure transformation was monitored by viscoelastic measurements, and the structural assignments of the intermediate states were performed by electron microscopy. The kinetics of transformation from macroscopically unaligned wormlike cylindrical microdomains to spherical microdomains arranged on a bcc lattice were extremely slow. The wormlike cylinder-to-sphere transition slowed with decreasing quench depth from the order−disorder transition. Additionally, these order−order kinetics were in quantitative agreement with those for the development of spherical microdomains from an initial disordered state. Further, during the initial induction time following a temperature jump from a wormlike cylindrical order to a spherical state, the sample exhibited liquidlike viscoelastic characteristics and structurally showed the absence of long-range order. In contrast, shear-aligned cylinders rapidly transformed to spheres, adopting a viscoelastic pathway distinct from that of the unaligned samples. The cylinder-to-sphere transition is thermotropically reversible, with the viscoelasticity-based kinetics of the sphere-to-cylinder transition being slower than the cylinder-to-sphere transition.

Introduction

Block copolymers form a range of novel microstructures depending on the length of the constituent blocks and the thermodynamic interaction between them. The microstructures range from alternating lamellae to cylinders to spheres with novel microstructures such as perforated lamellae, modulated lamellae, and gyroid intervening.[1,2] Block copolymers near the order−disorder transition (ODT) with appropriate relative chain lengths can also exhibit order−order transitions between these different microstructures.[3−5] The kinetics and pathway of such order−order transitions (OOT) have been predicted by a number of theoretical models,[6,7] and several experimental studies of order−order transitions have been reported recently.[8−20] Most of these experimental studies have been performed on shear-oriented block copolymers using small-angle neutron and X-ray scattering (SANS and SAXS, respectively) and viscoelastic measurements to probe the pathway associated with such transitions.

In this context, we recently reported[8] on the viscoelastic characterization of a cylinder-to-sphere OOT in a mixture of a di- and triblock copolymer system. We suggested that the cylinder-to-sphere transition observed was mediated by a long-lived poorly ordered structure that exhibited liquidlike viscoelastic properties. These appear to contradict previous studies of cylinder−sphere transitions performed on shear-aligned samples, where it has been shown that the transition occurs epitaxially and quite rapidly.[6,7,9−15] In this paper, we continue our study of the kinetics and pathway of the OOT in this mixture of highly asymmetrical matched diblock and triblock copolymer of polystyrene and poly(ethylene−butene-1) using transmission electron micrographs (TEM) and linear viscoelastic measurements. We present TEM evidence to confirm that the transition from wormlike cylinders to spheres in macroscopically unaligned samples is consistent with the pathway suggested by us earlier.[8] Further, we present viscoelastic characterization of the kinetics of the unaligned wormlike cylinder-to-sphere transition and the shear-aligned hexagonally packed cylinders-to-sphere transition and also describe the reverse sphere-to-cylinder transition. Finally, in the companion paper,[21] we describe the pathway of the shear-aligned cylinder-to-sphere transformation by SANS to provide an in-situ direct structural complementary study to that undertaken here and allow for a direct comparison to previous experimental studies.[9−15]

* Corresponding author. E-mail: ramanan@bayou.uh.edu.

Experimental Section

The sample examined in this study is a mixture of a matched triblock and diblock copolymer of polystyrene and poly(ethylene−butene-1), a commercial sample named Kraton G 1657 supplied by Shell Chemical Company. Detailed characterization of the sample was provided in a prior publication.[8] The salient features of the sample are the following: it contains 65 wt % triblock and 35 wt % diblock; it has an order−disorder transition temperature (T_{ODT}) of 195 ± 5 °C; and it exhibits a cylinder-to-sphere order−order transition (T_{OOT}) at 138 ± 3 °C (see detailed explanation in Results), with the spherical microphase being the stable microdomain structure for temperatures between T_{OOT} and T_{ODT}.

Melt state viscoelastic measurements were performed using a Rheometrics ARES rheometer with 25 mm diameter parallel plates and a transducer with an operating range of 0.2−2000 g cm. Samples of ∼2 mm thickness were vacuum molded at 180 °C for 30 min using a 1 ton load in a Carver press. After loading the sample in the rheometer, it was heated to 220 °C and held there for approximately 30 min in order to erase all prior thermomechanical history before cooling to a temperature below T_{ODT}. While cooling or heating the sample in the ordered state, it was always ensured that the normal force was close to zero, so as not to induce any macroscopic alignment of the sample.

10.1021/ma991841x CCC: $19.00
Published on Web 04/21/2000

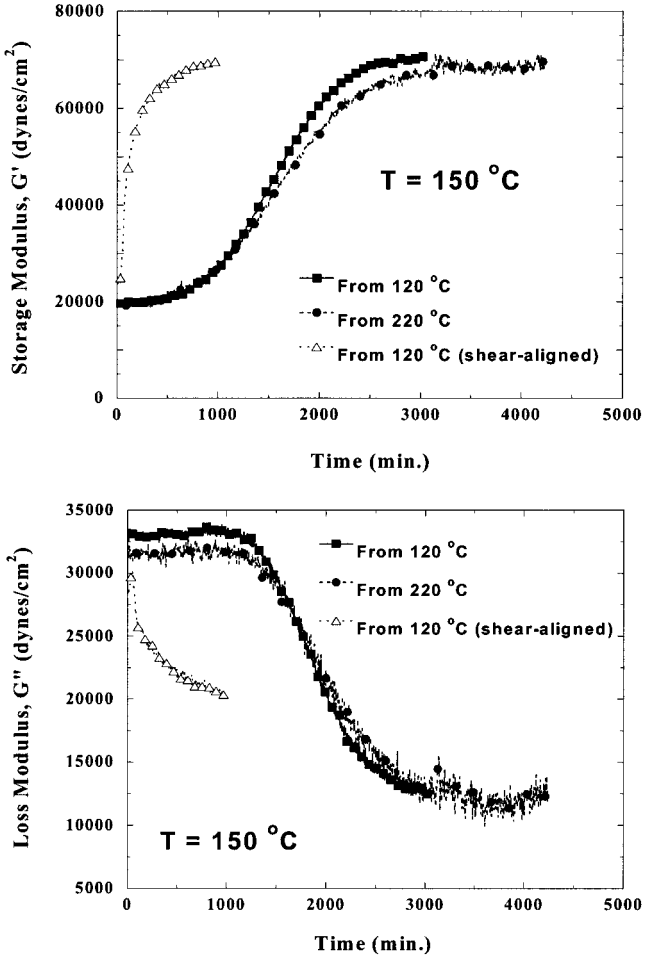

Figure 1. Temporal evolution of G' (a) and G'' (b) at a frequency $\omega = 0.03$ rad/s using a constant strain amplitude $\gamma_0 = 1.5\%$ at $T = 150$ °C from two separate states: cylindrically ordered ($T = 120$ °C) and disordered state ($T = 220$ °C). The initial moduli, the induction period, and growth phase of the development of the spherical structure for the disorder−sphere and cylinder−sphere transition are similar, suggesting that the cylinder-to-sphere transition is mediated by a poorly ordered state. Also shown is the growth of the spherical microdomains at $T = 150$ °C starting from shear-aligned cylinders, prepared by the prolonged application of large-amplitude oscillatory shear ($T = 120$ °C, $\omega = 0.01$ rad/s, $\gamma_0 = 100\%$, and time = 24 h).

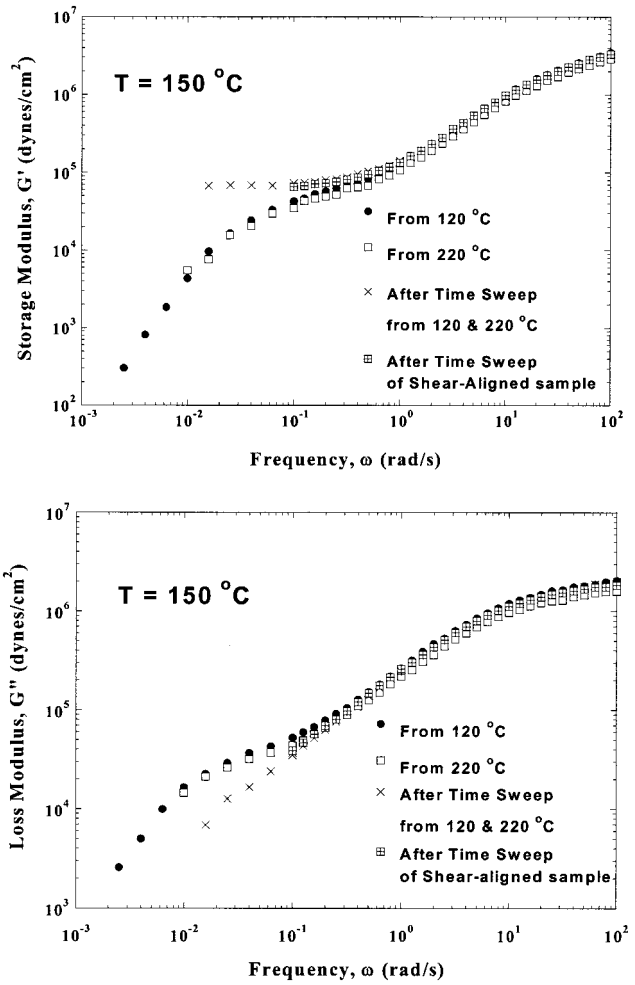

Figure 2. Plot of the frequency dependence of G' at $T = 150$ °C before and after the temporal evolution shown in Figure 1. The frequency dependence of G' goes from ω^2 to $\omega^{0.1}$ before and after the temporal evolution. Also shown is the data obtained at $T = 150$ °C immediately after a temperature jump from 220 °C. The data for the spherical state formed from an initial shear-aligned cylindrical state are similar to the ones obtained starting from unaligned wormlike cylinders and the disordered state, consistent with the lack of preservation of long-range single-crystal-like order under quiescent conditions for the spherical microdomains.

Dynamic isothermal frequency scans were performed by the successive application of an oscillatory strain of the form $\gamma(t) = \gamma_0 \sin(\omega t)$ as a function of logarithmically spaced frequencies (ω), and the resultant torque was converted to the in-phase storage modulus G' and the out-of-phase loss modulus G''. Only data ascertained to be linear, i.e., independent of strain amplitude γ_0, are shown in this paper. Temporal evolution of the order−order and the disorder−order transition was followed by monitoring the low-frequency linear viscoelastic properties as a function of time at constant strain amplitude γ_0, frequency ω, and temperature T. Typically, the sample reached thermal equilibrium in less than 10 min following a temperature jump. The conditions of ω and γ_0 were carefully selected to ensure a linear viscoelastic response with little or no changes in the microstructure as a result of the rheological testing, a torque signal that was considerably larger than the instrumental resolution, and a sampling time that was short but not at the cost of compromising the sensitivity of the kinetic data.

Samples for transmission electron microscopy were removed from the rheometer after testing and cooled rapidly (in liquid nitrogen or cold water) so as to preserve the microstructure of the test conditions. These samples were cryomicrotomed at −130 °C to obtain ultrathin sections (<100 nm thick) for TEM. These sections were stained with RuO_4 (a stain preferentially taken up by polystyrene) and then examined using a 160 keV Phillips EM 300 TEM as described earlier.[22]

Results

Structural Pathway. The temporal evolution of the dynamic moduli at 150 °C and constant ω and γ_0 to a final spherically ordered state starting from (i) an initially disordered state (220 °C) and (ii) a macroscopically unaligned wormlike cylindrically ordered state annealed at 120 °C for 48 h from an initial disordered state is shown in Figure 1. The storage modulus G' at low-frequency ($\omega = 0.03$ rad/s), starting from a small value which is independent of the initial state, increases dramatically after 600 min and reaches a significantly higher plateau value after over 2000 min. The frequency dependence of the moduli before and after the temporal development is shown in Figure 2. The liquidlike behavior in the initial incubation period, the sigmoidal-shaped time evolution of the moduli, and the remarkable similarity in the time dependence of the low-

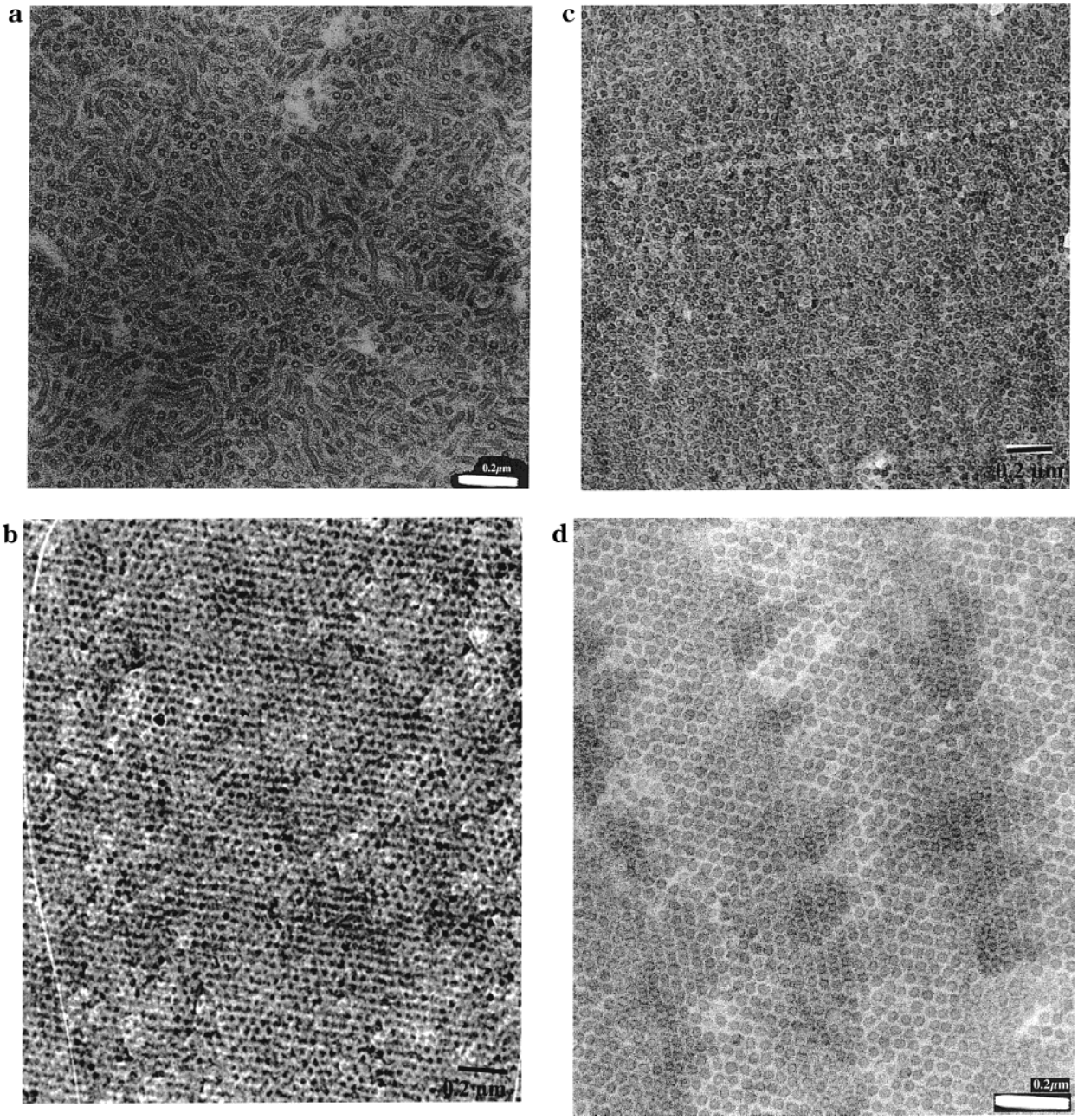

Figure 3. Transmission electron micrographs of unaligned samples after annealing for (a) 0, (b) 5, (c) 28, and (d) 74 h at 150 °C following a temperature jump from a macroscopically unaligned wormlike cylindrically ordered state (T = 120 °C). The samples were stained with RuO_4, which is preferentially absorbed by polystyrene. The dark regions correspond to the styrene-rich domains. The sample annealed at 120 °C (a) shows a wormlike cylindrical ordered microdomain, and the sample annealed at 150 °C (d) shows a spherically ordered microdomain. The micrograph b represents a macroscopically poorly ordered state, while in part c, the spherical microdomains are more clearly visible but not arranged on a well-defined lattice.

frequency G' during the ordering of the spheres onto a bcc lattice from either a disordered or a macroscopically unoriented wormlike cylindrically ordered state are noteworthy. On the basis of these observations, we had previously suggested[8] that the transformation from a cylindrically ordered state to a spherically ordered state was mediated by a poorly ordered state.

In Figure 3, the transition from a wormlike cylindrically ordered state to a spherically ordered state as examined by TEM is shown. Several tens of micrographs of each state were obtained, and the ones shown in Figure 3 are representative of the collection of micrographs for each condition examined. As noted earlier, samples were quenched by cooling with either liquid nitrogen or ice water to preserve the microstructure of the sample. Because of the proximity of the measuring temperatures to the glass transition of the polystyrene block and the relatively high molecular weight of the polymers, we expect good preservation of the microstructures using either cooling procedure. In fact, micrographs obtained from samples prepared using either cooling protocol were indistinguishable.

The micrographs corresponding to the initial cylindrical structure at 120 °C and the final bcc spherical microdomain structure at 150 °C (a and d, respectively) were shown in a previous paper and are reproduced here only for the sake of completeness. As noted previously,[8] the micrograph of the cylindrically ordered state shown is not that of the classical hexagonally packed honeycombed structure, and in fact, the structure shown

appears as "wormlike" cylinders with limited persistent length. However, the microphase separation and development of cylinders are clearly observed, and the linear viscoelastic response is indistinguishable from that of a well-defined hexagonally packed cylinder. Recent SAXS measurements have indicated that the primary intensity peak becomes Lorentzian when quenched to 120 °C from a disordered state and a simultaneous development of weak higher-order peaks.[23] Measurements carried out for a total annealing time of 96 h at these conditions revealed little or no change in the SAXS intensities and peak widths beyond a time of ~1 h after the quench. This wormlike cylindrical structure does not change with annealing time under quiescent conditions, and the development of such a structure is, in fact, consistent with a recent theory by Wang and co-workers.[24] They anticipate that, for systems quenched under quiescent conditions from a disordered state to temperatures well below the order−disorder transition, a cylindrical structure that is wormlike would be formed due to the development of long wavelength undulations during the reequilibration of the order parameter. Balsara and co-workers[25] have used SAXS and depolarized light scattering to study the development of cylindrical ordering in a polystyrene−polyisoprene diblock copolymer and have envisaged the formation of hexagonally packed cylinders with limited persistent length that straighten out by a second slow process. We suggest that for the systems examined here little or no straightening out process occurs under quiescent conditions within the time scale of the experiments (96 h). These wormlike cylindrically ordered materials, however, readily transform themselves to hexagonally closed-packed cylinders by the application of large-amplitude shear and develop into macroscopically aligned cylindrically ordered materials.

The series of micrographs in Figure 3 appears to support our hypothesis that the transformation from a macroscopically unaligned wormlike cylindrically ordered state to a bcc arranged spherically ordered state, in fact, proceeds via a macroscopically poorly ordered state. While clearly not erasing the microphase separation that exists between the polystyrene and poly(ethylene−butene-1) microdomains, the definitions of the individual microdomains are certainly blurred in Figure 3b. On the other hand, in Figure 3a, the cylindrical structures are well-defined microphase-separated structures and merely have limited persistence length. At a time corresponding roughly to the midpoint of the transformation of cylinders to spheres (based on the rheological signatures shown in Figure 1), the spherical microdomains appear fairly well defined, although not arranged on a well-defined lattice structure (Figure 3c). The lattice structure and regular ordering are clearly observed in the micrograph for a sample that has completely undergone the transformation and are shown in Figure 3d.

Kinetics of Ordering. The viscoelasticity-based kinetics of transformation to a *spherical state* at 140 °C (ω = 0.01 rad/s) from an initial disordered state are shown in Figure 4. Also shown in Figure 4 is the temporal evolution of the low-ω modulus for temperature jumps to 135 °C (cylindrically ordered), and these will be discussed below. Comparing Figures 4 and 1 (measurements conducted at roughly the same reduced frequency), the transformation at 140 °C is observed to be faster than that at 150 °C. However, the general

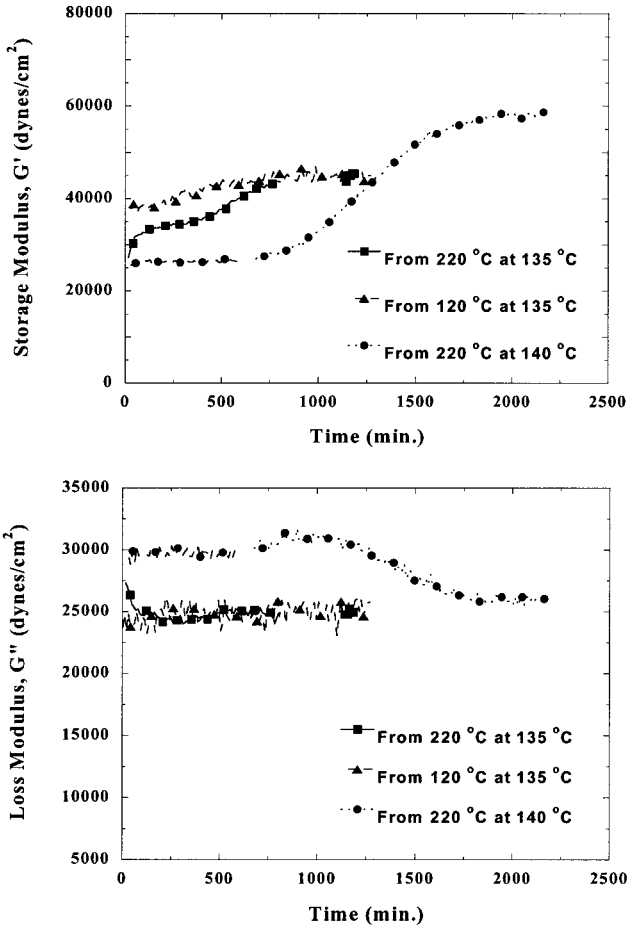

Figure 4. Temporal evolution of G' (a) and G'' (b) at a frequency ω = 0.01 rad/s using a constant strain amplitude γ_0 = 1.5% at T = 140 and 135 °C from the disordered state (T = 220 °C). The growth at 140 °C is qualitatively similar to the spherical growth observed at 150 °C. Also shown is the data at T = 135 °C after a jump from the wormlike cylindrically ordered state (T = 120 °C). There is no appreciable change in G' even after prolonged annealing. On the basis of these temporal developments, dynamic frequency scans, and TEM measurements, we establish that the sample exhibits an order−order transition at T_{OOT} = 138 ± 3 °C.

qualitative features for the transformation at the two temperatures are similar. The value of the storage modulus at the completion of the temporal evolution is similar, as would be expected on the basis of the near equivalence of the reduced frequencies and structural similarities.

The kinetics of the disordered to spherically ordered state and the wormlike cylindrical-to-spherical microdomains at 180 °C and ω = 0.1 rad/s are shown in Figure 5. The viscoelastic signatures of the transformation are qualitatively similar to those observed at 140 and 150 °C. However, the evolution at 180 °C is considerably slower than those at 140 and 150 °C. The temperature dependence of the kinetics of the growth of the spherical microdomains arranged on a bcc lattice from the disordered state is consistent with previous experiments,[9,26,27] where the kinetics were shown to be slowed down for temperatures closer to the order−disorder transition temperature. Further, our experiments suggest that the kinetics of the order−order transition are identical to the kinetics of the growth of the spherical state from a disordered state and primarily dictated by the distance from the order−disorder transition (i.e., $T - T_{ODT}$) and are speeded up with increasing

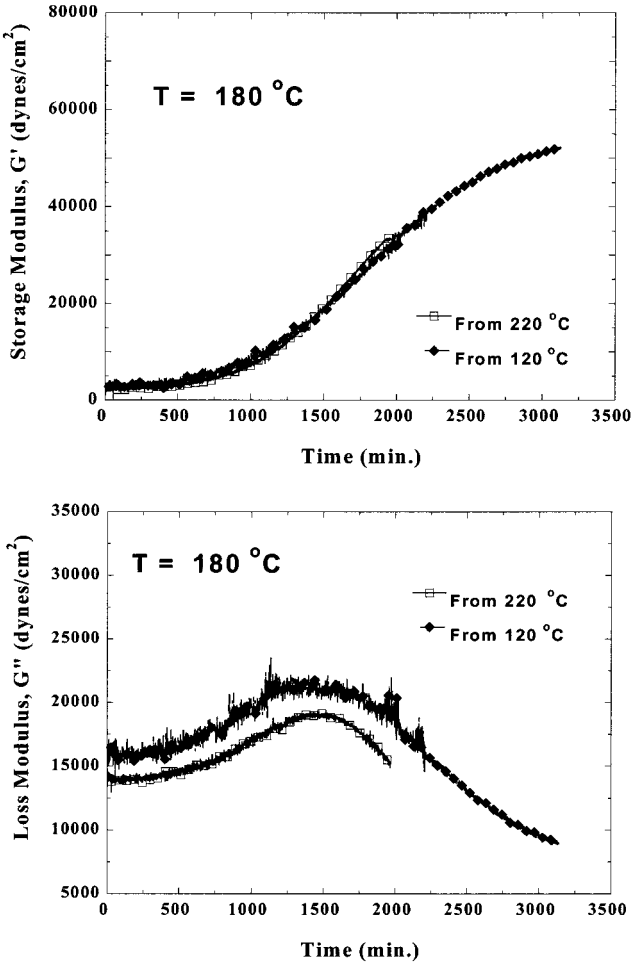

Figure 5. Temporal evolution of G' (a) and G'' (b) at a frequency $\omega = 0.1$ rad/s using a constant strain amplitude $\gamma_0 = 1.5\%$ at $T = 180$ °C from two distinct initial states: macroscopically unaligned wormlike cylindrically ordered ($T = 120$ °C) and the disordered state ($T = 220$ °C). The similarity in the initial modulus, the induction period, and growth phase of the development of the spherical structure, as observed earlier in Figure 1 at $T = 150$ °C, are noteworthy. However, the kinetics of the development of spheres arranged on a bcc lattice has slowed with decreasing quench depth.

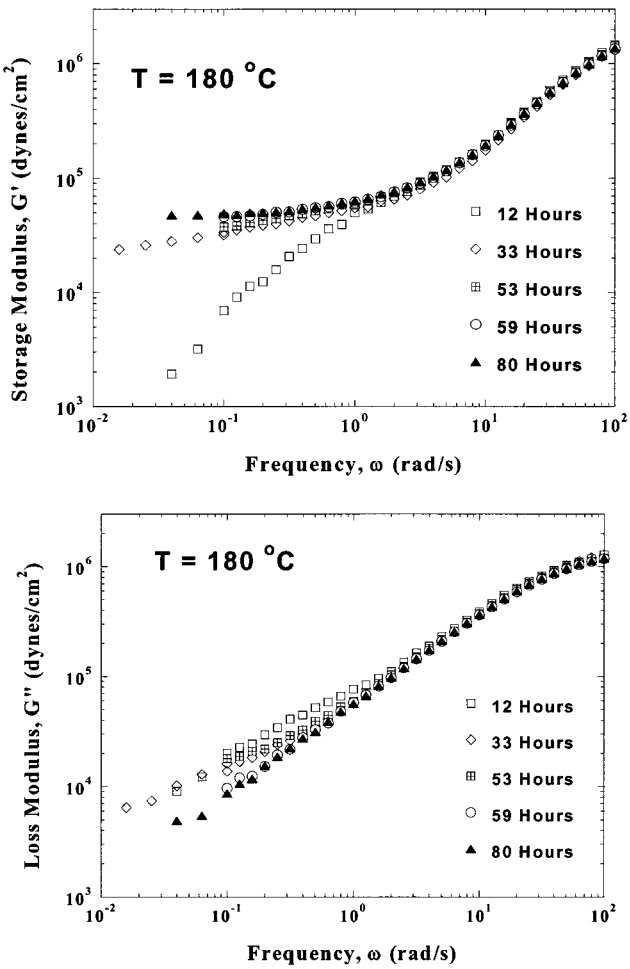

Figure 6. Isothermal frequency dependence of G' (a) and G'' (b) at 180 °C after a temperature jump from the well-equilibrated cylindrically ordered state ($T = 120$ °C) taken at intermediate time intervals as indicated in the figure. The frequency dependence of G' changes slowly: going from ω^2 at 12 h to $\omega^{0.3}$ after 33 h and finally to $\omega^{0.1}$ after 80 h.

magnitude of $|T - T_{ODT}|$. These results are consistent with our suggestion that the transition from the wormlike cylindrically orderedstate to a spherically ordered bcc microdomain state is mediated by a mesoscopically poorly ordered state.

The frequency dependence of the moduli at intermediate times during the wormlike cylinder-to-sphere order−order transition at 180 °C is shown in Figure 6. The data suggest that, during the incubation period, the sample exhibits liquidlike behavior, while further annealing results in a gradual transformation of the low-frequency viscoelastic response. These changes in the dynamic response are qualitatively consistent with those observed at 140 and 150 °C and are most clearly observed at 180 °C.

On the other hand, in Figure 4 is the evolution of the modulus for a quench to the cylindrical state at 135 °C from an initial disordered state. The time evolution of the moduli at 135 °C from an initially disordered state is qualitatively different from that observed for the development of the bcc spherical microdomains from a disordered state at 140, 150, and 180 °C. Figure 4 also shows the temporal evolution of G' and G'' at 135 °C for a temperature jump from a macroscopically unaligned wormlike cylindrical state at 120 °C. No significant changes in the moduli are observed, as would be expected for a temperature jump where no order−order transition is expected. Finally, TEM performed after the growth at 135 °C (not shown) suggests the existence of a *cylindrically ordered state.* It is on the basis of these experimental findings, i.e., bcc spheres at 140 °C and cylindrical microdomains at 135 °C, that we had previously assigned the order−order transition (T_{OOT}) to be 138 ± 3 °C.

On the other hand, the low-ω time-dependent development of G' and G'' for a sample quenched to 120 °C after annealing in the spherical state at 150 and 180 °C is shown in Figure 7. The data suggest that the transformation of cylinders to spheres is thermotropically reversible. On the basis of independent SANS and TEM measurements, we conclude that the sample after the prolonged annealing at 120 °C is, in fact, that of a cylindrically ordered sample. However, the sphere-to-cylinder transformation is considerably slower than the cylinder-to-sphere transition. Furthermore, as expected, the kinetics of the sphere-to-cylinder transition appear to be nearly independent of the temperature at which the annealing to the spherical state was carried out.

Figure 7 also shows the viscoelastic signature of the growth of the cylindrically ordered state at 120 °C from

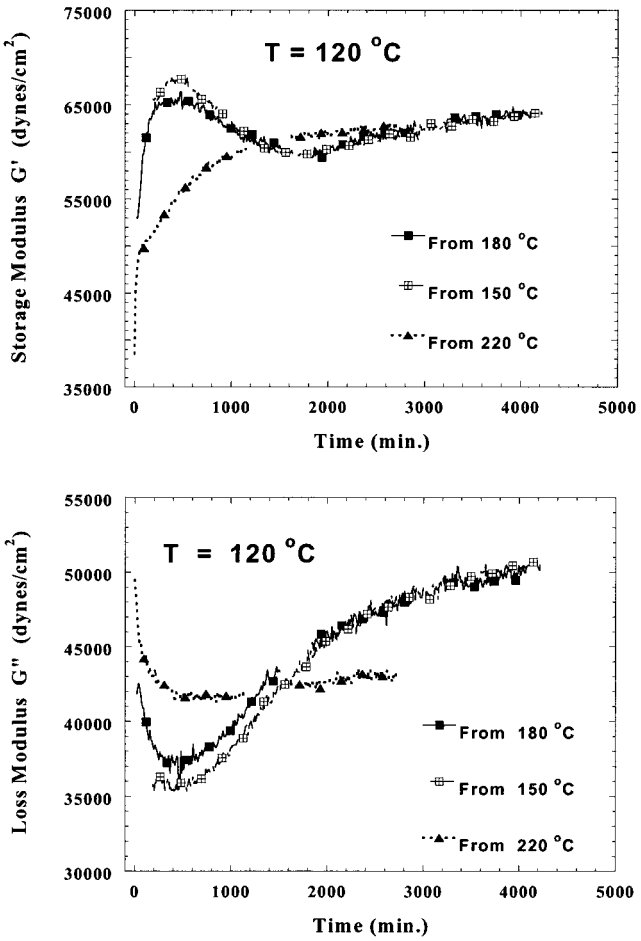

Figure 7. Temporal evolution of G' (a) and G'' (b) at a frequency $\omega = 0.01$ rad/s using a constant strain amplitude $\gamma_0 = 1.5\%$ at $T = 120$ °C from a spherically ordered state at $T = 180$ and 150 °C and from the disordered state ($T = 220$ °C). The reversible transition from spheres to cylinders is slower compared to the cylinder-to-sphere transition.

a disordered state. The kinetics and pathway for the evolution of the cylindrical state at 120 °C from a disordered state are different both qualitatively and quantitatively from those observed for the transition of bcc spheres to cylinders at the same temperature. The transformation kinetics, as inferred from the viscoelastic response for the disordered to cylindrically ordered state, is significantly faster than the transition from a spherical to cylindrical ordered state and could result from the possible additional mutual repulsion of the "hairy" spherical microdomains in the latter case.

Discussion

The results presented here suggest that the pathway from a macroscopically unoriented wormlike cylindrical state to a bcc ordered spherical state is mediated by a poorly ordered intermediate state that exhibits liquidlike viscoelastic characteristics. This pathway is consistent with the predictions of a time-dependent Landau−Ginzburg model of Qi and Wang.[6] By monitoring the amplitude of the hexagonal and bcc waves after a temperature jump from the cylindrical state to the spherical state, they observe that the hexagonal waves diminish rapidly, and the spherical waves become appreciable only after considerable time. On the other hand, Noolandi and co-workers[10] have also studied the cylinder-to-spherical transition using a theory of anisotropic fluctuations and suggest that the effect of the most unstable mode with small amplitudes leads to undulation of cylinders. Further, for larger amplitudes, the undulating cylinders break up to form ellipsoids on a bcc lattice. On the basis of the TEM micrographs of the intermediate states of the cylinder-to-sphere transition shown in Figure 3, we are unable to discern the presence of undulating cylinders as suggested by the work of Noolandi and observed by Lodge et al.[7] on a shear-aligned sample undergoing a cylinder-to-sphere transition. While the long-range order of hexagonal packing is absent, the microphase separation and formation of cylinders with limited persistent length are clearly evidenced in Figure 3a, and hence it would be expected that we should observe undulating cylinders in the intermediate states. In fact, micrographs from several samples during the initial incubation period prepared under different quenching protocols never exhibited a locally undulating cylindrical structure.

Most previous experimental studies[9−15] of cylinder-to-sphere order−order transitions have been performed on shear-oriented samples of either diblock or triblock copolymers. In those cases, the transformation was shown to be epitaxial with extremely fast kinetics. The epitaxial nature was confirmed by scattering measurements and the fast kinetics inferred from isochronal viscoelastic scans at reasonable heating rates. The kinetics reported here for the transition of unaligned wormlike cylinders to bcc ordered spheres, while being inconsistent with previous studies of shear-aligned cylinders-to-spheres transformations, are entirely consistent with previous studies of the development of spherical microdomains from an initially disordered state for highly asymmetric block copolymers.

To address this discrepancy in pathways, we have examined the kinetics of transformation for a sample that was shear-aligned in the cylindrical state ($T = 120$ °C, $\omega = 0.01$ rad/s, $\gamma_0 = 100\%$, and time = 24 h) and then subsequently annealed at a temperature of 150 °C. The temporal evolution is shown in Figure 1 and is seen to be qualitatively different from that obtained from a macroscopically unoriented sample. The transformation is rapid and the initial incubation period, where the unoriented sample appears poorly ordered, if it exists, is too short to be observed in the viscoelastic measurements. In the accompanying paper,[21] we examine the pathway for the order−order transition for shear-oriented samples using SANS and show that, for the case of shear-aligned cylinders, the transformation while still being mediated by a poorly ordered state does in fact lead to an epitaxial growth of the bcc microdomains from the hexagonally closed packed cylinders. The frequency dependence of the moduli for a bcc spherical microdomain material obtained from the shear-aligned cylinders is identical to that of a spherical sample having been formed from an initially unoriented cylindrical state (Figure 2). The lack of preservation of long-range order under quiescent conditions after shear alignment in a cubic symmetry microstructure is well-known, and the spherical state found here does not maintain a single-crystal-like long-range order after cessation of flow. It thus appears that, while the transformation kinetics of the cylinder-to-sphere transition is dependent on the state of long-range order of the initial cylindrical microdomains, the pathway and the

mediation by a poorly ordered state appear to be common features.

Another issue that might contribute to the unusual cylinder-to-sphere kinetics observed here is the fact that we are using a matched diblock and triblock copolymer blend. However, some preliminary measurements in our laboratory on the fractionated diblock and triblock copolymers of the sample examined here exhibit *qualitatively* similar features to those presented here. Further, Lodge and co-workers[7] have examined the order−order and order−disorder transition in highly asymmetric polystyrene−polyisoprene matched diblock and triblock copolymers using SAXS measurements on oriented samples. While the temperatures of the transitions were slightly different for the two architectures, no substantial slowing down was observed in the case of the triblocks. In fact, previously Bates and co-workers[18,19] employed two diblock copolymers to generate a block copolymer system capable of undergoing gyroid-to-lamellae transition and found no unusual features regarding the kinetics and pathway as a result of the blending. Thus, we conclude that the polydispersity has little influence on the pathway of the order−order transition reported in this paper.

Additionally, it is possible that the lack of long-range order characteristic of the cylindrically ordered microdomains might contribute to the unusual cylinder-to-sphere transition kinetics and pathway observed here. The samples were typically annealed at a temperature of 120 °C for 24−48 h in all cases before any kinetic studies of the cylinder-to-sphere transition were performed. The linear viscoelastic behavior typically showed no change with time and was characteristic of cylindrically ordered block copolymers (i.e., at low frequencies G' and $G'' \propto \omega^{1/3}$)[28] after 24 h of annealing at 120 °C. Repeat measurements carried out with annealing times of 24, 48, and 96 h exhibited no change in the pathway or the kinetics of the order−order transition. The formation of wormlike cylinders is anticipated on the basis of a recent theory by Wang and co-workers[24] where they suggest that, with increased quench depth, a long wavelength undulation of the cylinders accompanies the reequilibration of the order parameter. Balsara and co-workers[25] have also recently shown that, for the growth of cylinders from an initially disordered state and for large quench depths, the kinetics appear to be spinodal in nature, and cylinders with short persistent lengths are grown that straighten out by a much slower process. Additionally, on the basis of SANS measurements presented in the accompanying paper,[21] it is clear that while the kinetics of the cylinder-to-sphere transition are dependent on the large-scale order in the cylindrical state, the mechanism where a poorly ordered state mediates the transition is independent of this initial structure. We return to the possible molecular arguments for the pathway observed for the cylinder-to-sphere transformation in the accompanying paper,[21] where we present the in-situ structural evidence for the pathway using SANS on shear-aligned cylinders.

The kinetics of the ordering to a spherical state from either a disordered state or a macroscopically unaligned wormlike cylindrically ordered state are consistent with previous studies of the evolution of a spherical state from the disordered state.[9−15,26,27] The storage modulus exhibits a sigmoidal time dependence, while the loss modulus exhibits time dependencies which are a function of the reduced frequency at which the development of spherical microdomains is monitored. For 140 and 150 °C, where the reduced frequencies of measurement are roughly equal, the data for G'' have similar shapes, i.e., a sigmoidal decrease. However, at 180 °C the measurements were carried out at a higher reduced frequency, and the loss modulus exhibits a maximum (Figure 5b) and not the sigmoidal time dependence. Thus, we focus on the storage modulus G' and the complex modulus G^* to quantitatively analyze the temporal behavior of the OOT from cylinders to spheres. The time evolution of G' and G^* can be adequately fitted using the Avrami equation, of the form

$$G'(t) = G'(0) + [G'(\infty) - G'(0)]\left[1 - \exp\left(-\frac{t}{\tau}\right)^{\beta}\right] \quad (1)$$

where $G'(t)$, $G'(0)$, and $G'(\infty)$ are the values of the storage modulus at a time t, initially at $t = 0$, and the final saturated condition, respectively. An analogous expression is used to fit the complex modulus G^*. The parameter τ represents a characteristic time for the growth process and has been labeled the half-time in previous studies.[9,26,27] The fitted values of τ and β as a function of temperature are presented in Table 1. As expected from the data presented in Figures 1, 4, and 5, the characteristic time τ increases with increasing temperature. Previous studies have suggested[9,26] that the value of β is significantly lower near the order−disorder temperature ($T_{ODT} - T \leq 3$ °C) as compared with those for deeper quench depths. For deep quenches, the value of β was found to remain roughly constant at approximately 3. The value of β at 140 °C is considerably different and might suggest a possible influence of the order−order transition on the value of β and the kinetics of the transformation.

Table 1. Fit of Temporal Evolution from the Disordered State

	G'		G^*	
temp (°C)	τ (min)	β	τ (min)	β
140	1350	4.6	1350	4.2
150	1550	3.1	1600	3.2
180	1930	3.2	2040	3.1

On the other hand, the transformation from spheres to cylinders, based on the viscoelastic response shown in Figure 7, appears not to proceed via a mesoscopically poorly ordered state. The viscoelastic response during this transformation is nonmonotonic and exhibits a peak in the storage modulus and a concomitant trough in the loss modulus at short times. Frequency scans at intermediate times (not shown) during the transition showed no dramatic changes in magnitude of the moduli or their slopes even at the lowest frequencies examined. The sphere-to-cylinder transition, based on the viscoelastic signatures, is slower than the corresponding cylinder-to-sphere transition. Intuitively, since cylindrical microphase-separated structures are formed by a coalescence of the bcc arranged spheres which are expected to hydrodynamically repel each other despite a thermodynamic driving force favoring coalescence, we expect a slowing down of the sphere-to-cylinder transition. Additionally, Noolandi and co-workers[10] suggest that the sphere-to-cylinder transition proceeds via a modulated layered state and could also lead to a slowing down of the kinetics. Unfortunately, on the basis of the observed rheological response and the absence of scattering or microscopy information, we cannot shed more light on the pathway of the sphere-to-cylinder transition. We are

currently pursuing measurements of the structural changes associated with the sphere-to-cylinder transition using SANS and TEM measurements.

Concluding Remarks

The results presented in this paper suggest that the pathway for the transition of unaligned wormlike cylinders to spheres arranged on a bcc lattice is mediated by a poorly ordered state with liquidlike flow characteristics. The kinetics of the ordering transition to a spherical ordered state from a disordered state or from a wormlike cylindrical ordered state are slowed with decreasing quench depth from the ODT. Micrographs of the intermediate state in the evolution of wormlike cylinders to spheres appear to be consistent with the viscoelastic signatures reported here: poor long-range order for the sample in the initial incubation period of the transition, followed by the development of spherical microdomains without long-range order during the growth phase, with subsequent perfection of the ordered spherical microdomains onto a regular bcc lattice. This structural development is consistent with the theoretical time-dependent Landau−Ginzburg model suggested by Qi and Wang[6] for the cylinder-to-sphere transition. In contrast, for shear-aligned cylinders, the transformation to spheres is hastened, and the viscoelastic pathway is distinctly different from that observed for the macroscopically unoriented cylindrical state. The shear-aligned materials, in fact, exhibit epitaxial transformation from cylinders to spheres, and the pathway for that transition as studied by SANS is presented in the companion paper.[21] In that work, we clearly demonstrate that even for the transformation of shear-aligned cylinders to spheres, a poorly ordered state mediates the transition, and this pathway is not a result of the wormlike cylindrical structure formed under quiescent conditions here.

Further, the order−order transformation is thermotropically reversible with the transformation from spheres to cylinders being slower than the cylinder-to-sphere transition. Finally, the pathway of the spherical-to-cylindrical transition, at least on the basis of the viscoelastic signatures, is not mediated by a poorly ordered state. The precise microstructural pathway of this reverse sphere-to-cylinder transition is currently being investigated using SANS measurements on shear-aligned samples.

Acknowledgment. We thank Profs. Wang, Lodge, and Balsara for useful discussions and Mr. J. W. Ball for assistance with the TEM measurements. Critical discussions with Dr. Silva are also gratefully acknowledged. We also thank a referee of the manuscript whose comments have been invaluable. Funding from the Research Initiation Grant from the University of Houston and the Energy Laboratory at the University of Houston is gratefully acknowledged.

References and Notes

(1) Bates, F. S.; Fredrickson, G. H. *Annu. Rev. Phys. Chem.* **1990**, *41*, 525.
(2) Fredrickson, G. H.; Bates, F. S. *Annu. Rev. Mater. Sci.* **1996**, *26*, 501.
(3) Leibler, L. *Macromolecules* **1980**, *13*, 1602.
(4) Fredrickson, G. H.; Helfand, E. *J. Chem. Phys.* **1987**, *87*, 697.
(5) Matsen, M. W.; Bates, F. S. *Macromolecules* **1996**, *29*, 1091.
(6) Qi, S.; Wang, Z.-G. *Phys. Rev. Lett.* **1996**, *76*, 1679. Qi, S.; Wang, Z.-G. *Phys. Rev. E* **1997**, *55*, 1682.
(7) Ryu, C. Y.; Lee, M. S.; Hajduk, D. A.; Lodge, T. P. *J. Polym. Sci., Part B: Polym. Phys.* **1997**, *35*, 2811. Ryu, C. Y.; Vigild, M. E.; Lodge, T. P. *Phys. Rev. Lett.* **1998**, *81*, 5354. Ryu, C. Y.; Lodge, T. P. *Macromolecules* **1999**, *32*, 7190.
(8) Modi, M. A.; Krishnamoorti, R.; Tse, M. F.; Wang, H.-C. *Macromolecules* **1999**, *32*, 4088.
(9) Hajduk, D. A.; Tepe, T.; Takenouchi, H.; Tirrell, M.; Bates, F. S.; Almdal, K.; Mortensen, K. *J. Chem. Phys.* **1998**, *108*, 326.
(10) Laradji, M.; Shi, A. C.; Desai, R. C.; Noolandi, J. *Phys. Rev. Lett.* **1997**, *78*, 2577. Laradji, M.; Shi, A. C.; Noolandi, J.; Desai, R. C. *Macromolecules* **1997**, *30*, 3242.
(11) Sakurai, S.; Hashimoto, T. *Macromolecules* **1996**, *29*, 740. Sakurai, S.; Umeda, H.; Taie, K.; Nomura, S. *J. Chem. Phys.* **1996**, *105*, 8902. Sakurai, S.; Kawada, H.; Hashimoto, T.; Fetters, L. *Macromolecules* **1993**, *26*, 5796. Sakurai. S.; Hashimoto, T.; Fetters, L. *J. Polym. Prepr., Jpn., Soc. Polym. Sci., Jpn.* **1991**, *40*, 770.
(12) Koppi, K. A.; Tirrell, M.; Bates, F. S.; Almdal, K.; Mortensen, K. *J. Rheol.* **1994**, *38*, 999.
(13) Hamley, I. W.; Gehlsen, M. D.; Khandpur, A. K.; Koppi, K. A.; Rosedale, J. H.; Schulz, M. F.; Bates, F. S.; Almdal, K.; Mortensen, K. *J. Phys. II* **1994**, *4*, 2161.
(14) Hajduk, D. A.; Gruner, S. M.; Rangarajan, P.; Register, R. A.; Fetters, L. J.; Honeker, C.; Albalak, R. J.; Thomas, E. L. *Macromolecules* **1994**, *27*, 490.
(15) Sakamoto, N.; Hashimoto, T. *Macromolecules* **1998**, *31*, 3292. Sakamoto, N.; Hashimoto, T. *Macromolecules* **1998**, *31*, 8493.
(16) Förster, S.; Khandpur, A. K.; Zhao, J.; Bates, F. S.; Hamley, I. W.; Ryan, A. J.; Bras, W. *Macromolecules* **1994**, *27*, 6922.
(17) Almdal, K.; Koppi, K. A.; Bates, F. S.; Mortensen, K. *Macromolecules* **1992**, *25*, 1743.
(18) Gehlsen, M. D.; Almdal, K.; Bates, F. S. *Macromolecules* **1992**, *25*, 939.
(19) Schulz, M. F.; Bates, F. S.; Almdal, K.; Mortensen, K. *Phys. Rev. Lett.* **1994**, *73*, 86.
(20) Kim, J. K.; Lee, H. H.; Gu, Q.-J.; Chang, T.; Jeong, Y. H. *Macromolecules* **1998**, *31*, 4045.
(21) Krishnamoorti, R.; Silva, A. S.; Modi, M. A.; Hammouda, B. *Macromolecules* **2000**, *33*, 3803.
(22) Tse, M. F.; Wang, H.-C.; Shaffer, T. D.; McElrath, M. C.; Modi, M.; Krishnamoorti, R. Presented at 152nd Meeting of Rubber Division, American Chemical Society, Cleveland, Oct 21−24, 1997; paper no. 17.
(23) Krishnamoorti, R. Manuscript in preparation.
(24) Qi, S.; Wang, Z.-G. *J. Chem. Phys.* **1999**, *111*, 10681.
(25) Balsara, N. P.; Garetz, B. A.; Newstein, M. C.; Bauer, B. J.; Prosa, T. J. *Macromolecules* **1998**, *31*, 7668.
(26) Adams, J. L.; Quiram, D. J.; Graessley, W. W.; Register, R. A.; Marchand, G. A. *Macromolecules* **1996**, *29*, 2929.
(27) Floudas, G.; Ulrich, R.; Wiesner, U. *J. Chem. Phys.* **1999**, *110*, 652. Floudas, G.; Pispas, S.; Hadjichristidis, N.; Pakula, T.; Erukhimovich, I. *Macromolecules* **1996**, *29*, 4142. Floudas, G.; Fytas, G.; Hadjichristidis, N.; Pitsikalis, M. *Macromolecules* **1995**, *28*, 2359. Floudas, G.; Hadjichristidis, N.; Iatrou, H.; Pakula, T.; Fischer, E. W. *Macromolecules* **1994**, *27*, 7735.
(28) Colby, R. C. *Rev. Polym. Phys.* **1999**, *1*, 1.

MA991841X